Binding of calcium in the EF-hand of *Escherichia coli* lytic transglycosylase Slt35 is important for stability

Erik J. van Asselt, Bauke W. Dijkstra*

BIOSON Research Institute and Laboratory of Biophysical Chemistry, University of Groningen, Nijenborgh 4, 9747 AG Groningen, The Netherlands

Received 15 June 1999; received in revised form 30 July 1999

Abstract The *Escherichia coli* lytic transglycosylase Slt35 contains a single metal ion-binding site that resembles EF-hand calcium-binding sites. The Slt35 EF-hand is only the second observation of such a domain in a prokaryotic protein. Two crystal structures at 2.1 Å resolution show that both Ca^{2+} ions and Na^{+} ions can bind to the EF-hand domain, but in subtly different configurations. Heat-induced unfolding studies demonstrate that Ca^{2+} ions are preferentially bound, and that only Ca^{2+} ions significantly increase the melting temperature of Slt35. This shows that the EF-hand calcium-binding domain is important for the stability of Slt35.

Key words: EF-hand; Lytic transglycosylase; Thermostability; Crystal structure; Calcium; *Escherichia coli*

1. Introduction

For many proteins, calcium is essential for folding, (thermo)stability, (re)activity and function. One of the most familiar calcium-binding motifs that nature has designed is the EF-hand, first discovered in carp parvalbumin B [1] and subsequently observed in many other proteins [2]. The EF-hand fold consists of a helix-loop-helix module with the two helices forming the finger (helix E) and the thumb (helix F) of a right hand. The loop between helices E and F contains the EF-hand consensus sequence. Oxygen atoms from the residues in positions 1, 3, 5, 7, 9 and 12 of this motif coordinate the calcium ion in a pentagonal bipyramidal fashion [3].

EF-hand calcium-binding domains are rare among prokaryotic proteins, and have so far only been observed in the periplasmic glucose/galactose-binding proteins (GBP) from *Escherichia coli* [4] and *Salmonella typhimurium* [5]. However, recently a metal ion-binding module was identified in the crystal structure of the *E. coli* lytic transglycosylase Slt35 that also resembles the EF-hand domains [6,7]. Slt35 is a naturally occurring, soluble proteolytic fragment (residues 40–361) of the 40 kDa membrane-bound lytic transglycosylase B (MltB) [8,9], which is one of the six identified lytic transglycosylases in *E. coli*. These enzymes catalyse the cleavage of the β(1,4)-glycosidic bond between *N*-acetylmuramic acid and *N*-acetylglucosamine residues in peptidoglycan with concomitant formation of a 1,6-anhydro bond between the C1 and O6 atoms of the *N*-acetylmuramic acid residue. They are believed to function as space makers to allow the insertion of new peptidoglycan material into the cell wall during growth [10] and as pore makers in the peptidoglycan layer to allow transport of DNA and proteins across the cell wall [11]. Moreover, they have been proposed to act as cell wall zippers during cell division [12].

The resemblance of the metal ion-binding site in Slt35 to the EF-hand calcium-binding sites suggested that a calcium ion could be present in the native structure. The average ion-ligand distance was 2.4 Å, which is typical for calcium-oxygen distances. However, some conspicuous differences with other EF-hand calcium-binding domains are noticeable. Firstly, the EF-hand loop of Slt35 does not contain the usual 12 residues, but it consists of 15 residues (residues 237–251), in which the bidentate ligand at position 12 has moved to position 15 (Asp-251). Secondly, the metal ion was coordinated by only six oxygen ligands and not seven as normally observed for EF-hand calcium-binding domains [4,13]. Thirdly, the ligands of the metal ion did not have the typical pentagonal bipyramidal configuration, but a distorted octahedral geometry. Fourthly, refinement of the metal ion as a calcium resulted in an atomic displacement parameter that was almost twice the average *B*-factor of the ligands. As no calcium was present in the crystallisation solutions, the identity of the metal ion bound in the EF-hand domain remained elusive. Here we present conclusive evidence that under natural conditions calcium is present in Slt35. Furthermore, calcium but not other mono- or divalent cations enhances the protein's thermostability.

2. Materials and methods

2.1. Crystal soaking experiments and data collection

The Slt35 protein was isolated [8] and subsequently crystallised in the presence of a bicine-NaOH buffer (pH 7.8) [6]. To establish that the metal ion-binding site of Slt35 can bind calcium, two X-ray diffraction data sets were collected from a single crystal. The first data set (Slt35-Na) was obtained from a native crystal, which had first been soaked for 30 min in a 0.1 M bicine-NaOH buffer, pH 8.0, with 5% PEG20K, and subsequently for 1 min in a cryo-protectant solution consisting of 50 μl of this buffer and 50 μl of a 87% glycerol solution in water. Data collection was carried out at 120 K. Next, the crystal was thawed and thoroughly washed in a 0.1 M Tris-HCl buffer, pH 8.0, with 5% PEG20K and 1 mM $CaCl_2$, in order to remove the Na^{+} ions. The washing solution was refreshed four times over a period of 2 h. After soaking for 1 min in a cryo-protectant solution (50 μl 0.1 M Tris-HCl buffer, pH 8.0, with 5% PEG20K, 1 mM $CaCl_2$ and 50 μl of a 87% glycerol solution in water) the second diffraction data set (Slt35-Ca) was obtained at 120 K as well. All diffraction data were collected in house on a DIP 2030H image plate (MacScience) using Cu Kα radiation from a Nonius FR591 rotating anode generator with Franks' mirrors. Data were processed with DENZO and SCALEPACK [14] and the measured intensities were converted to structure factor amplitudes with programs from the Groningen BIOMOL software package. Data collection statistics can be found in Table 1.

*Corresponding author. Fax: (31) (50) 363 4800.
E-mail: bauke@chem.rug.nl

PII: S0014-5793(99)01198-9

Table 1
Data collection and refinement statistics

A. Data collection		
Data set	Slt35-Na	Slt35-Ca
Metal ion bound in EF-hand domain	Na^+	Ca^{2+}
Space group	$P\ 2_12_12_1$	$P\ 2_12_12_1$
Cell dimensions (*a, b, c* in Å)	58.5, 67.8, 98.7	58.4, 67.8, 99.1
R_{merge} (%) (last shell)[c]	6.4 (19.1)	6.3 (27.4)
Resolution limit (Å)	2.10	2.10
Completeness (%) (last shell)	92.1 (94.4)	92.6 (91.0)
B. Refinement		
Resolution range	20.0–2.10	20.0–2.10
Number of reflections	21 174	21 500
work set	19 099	19 359
test set	2 075	2 141
R_{all} (%)[a]	16.1	16.2
R_{work} (%))[a]	15.8	15.9
R_{free} (%))[a]	21.0	20.6
Est. error from cross-validated		
Luzzati plot	0.24	0.23
SigmaA plot	0.20	0.22
RMSD)[b]		
Bond lengths	0.009	0.009
Bond angles	1.3	1.3
Dihedral angles	22.3	22.2
Improper angles	1.21	1.24
Average *B*-factor (Å^2)		
from Wilson plot	6.2	9.4
All atoms	16.1	17.6

[a] R-factor $= \Sigma_{hkl}||F_{obs}|-|F_{calc}||/\Sigma_{hkl}|F_{obs}|$. R_{all} is the R-factor after a final refinement cycle with inclusion of all reflections with $F>0$ (= combined work and test sets). R_{work} and R_{free} are defined for reflections with $F>0$.
[b] With respect to the Engh and Huber parameters [27].
[c] $R_{merge} = \Sigma_{hkl}|I-\langle I\rangle|/\Sigma_{hkl}I$.

2.2. Refinement

The starting model for the refinement was native Slt35 including all solvent molecules, which had previously been refined at 1.7 Å resolution to an R_{work} of 17.9% and R_{free} of 21.5%. For the refinement of Slt35-Na and Slt35-Ca, test set reflections were selected from the test set used for the refinement of the native data. After rigid-body refinement (8.0–3.5 Å resolution), the models were refined in several cycles of Powell energy minimisation, occupancy refinement of alternate side chain conformations, overall and individual *B*-factor refinement with X-PLOR version 3.843 [15] and manual rebuilding with the program O [16]. In the first refinement cycles, a low resolution cut-off of 6 Å was applied, but towards the end of the refinement the cut-off was set to 20.0 Å and a bulk solvent correction was used. The application of resolution-dependent and sigma weighting schemes ($1/\sigma^2$) resulted in lower R_{free} values and smaller differences between R_{work} and R_{free}. The last refinement cycle was repeated with all data including the test set. The final refinement statistics are summarised in Table 1. Stereochemistry was inspected with the programs PROCHECK [17] and WHATCHECK [18]. Coordinates and structure factors have been deposited with the Protein Data Bank. The PDB entries are 1QDR for Slt35-Na and 1QDT for Slt35-Ca.

2.3. Spectroscopic measurements

Heat-induced unfolding of Slt35 was studied by far-UV circular dichroism (CD) and by fluorescence spectroscopy. For these experiments, 7 mg/ml of Slt35 was dialysed overnight against a solution of 50 mM Tris-HCl (pH 7.4) and 2% isopropanol (to prevent precipitation). For the actual measurements this stock solution was diluted to a protein concentration of 70 μg/ml. Tris-HCl solutions were chosen, rather than the phosphate buffer preferred for CD spectroscopy, to prevent precipitation of calcium phosphate and to avoid the presence of sodium or potassium ions. To study the effect of different metal ions on unfolding, 1, 10 or 100 mM NaCl, $MgCl_2$, KCl or $CaCl_2$ was added to the protein solution (see Section 3). Far-UV CD and fluorescence measurements were performed on an Aviv 62A DS circular dichroism spectrometer equipped with a thermoelectric sample holder for adequate temperature control. CD data were recorded in a 2 mm path length cell. Temperature scans between 25° and 75°C were performed by increasing the temperature in steps of 1°C, during which the unfolding of Slt35 was monitored by CD at 222 nm recording the signal for 20 s and by fluorescence at 305–500 nm after excitation of tryptophan residues at 295 nm.

3. Results and discussion

3.1. Structure determination of the Slt35-metal ion complexes

The crystal structure of Slt35 has been recently determined at 1.7 Å resolution [6]. The protein is built up of three well-defined domains named the alpha, beta and core domains (Fig. 1). Residues from the core domain form a large and deep groove, where the peptidoglycan substrate is supposed to bind, and where the active-site residue Glu-162 is located. In the core domain, an EF-hand helix-loop-helix module was found consisting of α-helices H10 (residues 228–234) and H11 (residues 249–262), with residues 237–251 constituting the metal ion-binding loop. However, the nature of the metal ion bound in this domain was not clear. Therefore we carried out two different soaking experiments with the same crystal. In the presence of 0.1 M bicine-NaOH pH 8.0 (Slt35-Na; see Table 1 for pertinent details on the structure determination), the metal ion in the EF-hand module was best refined as a Na^+ ion, as judged from the similarity of its atomic displacement parameter to those of the coordinating atoms. The resulting structure is very similar to the high-resolution native Slt35 structure (Table 2).

However, after extensively washing the crystal to remove the Na^+ ions, and after subsequent soaking of the crystal in a 1 mM Ca^{2+}-containing solution, a $(|F_{obs}(Ca^{2+})| - |F_{obs}(Na^+)|)$ difference Fourier electron density map showed a 22σ peak at the metal-binding site (Fig. 2C), indicating that the bound Na^+ ion had been replaced by a Ca^{2+} ion. After refinement, this Ca^{2+} ion had acquired an atomic displacement parameter that is similar to those of its ligands (Table 3). From Table 2 it can be seen that the structures of native Slt35, Slt35-Na and Slt35-Ca do not differ significantly, except for some small differences in the metal ion-binding site. Analysis of the *B*-factor distribution in the Slt35-Na and Slt35-Ca structures shows that the average *B*-factors are also comparable for the structures. In the only other prokaryotic protein with a calcium-binding site that resembles the EF-hand calcium-binding site, the galactose-binding protein of *E. coli*, calcium also induced only local conformational changes [19].

3.2. Coordination of the metal ions

In both Slt35-Na and Slt35-Ca, the metal ion is coordinated by six protein oxygen atoms (Oδ1 of Asp-237, Oγ of Ser-239, Oδ1 of Asp-241, O of His-243, Oδ1 and Oδ2 of Asp-251), with an average metal ion-ligand distance of 2.4–2.5 Å (Fig. 2 and Table 3A). Nevertheless, distinct differences between the Na^+ and Ca^{2+} complexed Slt35s can be observed. In the Slt35-Ca structure, a seventh ligand is a water molecule at 2.4 Å distance, whereas this solvent molecule is much further away in the Slt35-Na structure (3.4 Å). The positions of the Na^+ and Ca^{2+} ions differ by 0.7 Å (Table 2), and the main chain ψ angles for Asp-237 and His-243, and the side chain $\chi 2$ angles of Asp-237, Asp-241, Asp-248 and Asp-251 are slightly

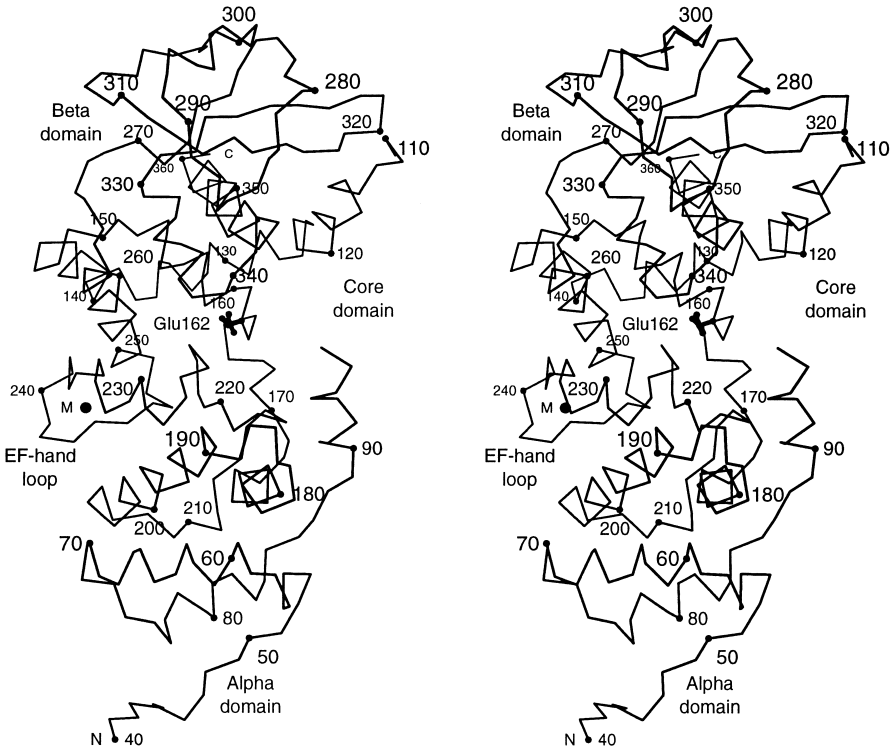

Fig. 1. Stereo view of a Cα trace of Slt35. The alpha domain (residues 40–98 and 170–215) and beta domain (residues 270–329) are respectively found at the bottom and top of Slt35 in the orientation as depicted in the figure. The core domain with the active site residue Glu-162 in bold is sandwiched between the alpha and beta domains and contains residues 109–169, 216–269 and 330–361. The metal ion-binding site (M) is located in a loop of 15 residues (residues 237–251) between α-helices H10 (residues 228–234) and H11 (residues 249–262). The figure was prepared with MOLSCRIPT [23].

different (Table 3B). These differences result in a distorted octahedral coordination of the metal ion in the Slt35-Na structure, and in a pentagonal bipyramidal geometry in the Slt35-Ca structure. Thus, it appears that both Na^+ and Ca^{2+} ions can bind in the EF-hand module of Slt35. The Slt35-Na structure is very similar to the native Slt35 structure (data not shown), suggesting that a Na^+ ion was present in the latter structure as well.

3.3. Heat-induced unfolding of Slt35

To study the functional importance of various monovalent and divalent cations for Slt35, the heat-induced unfolding of Slt35 was followed by CD and fluorescence spectroscopy (Fig. 3). The CD spectrum of Slt35 shows strong signals around 197, 209 and 222 nm (Fig. 3A). The spectrum is typical for α-helical proteins (50% of the Slt35 residues are in an α-helical conformation) and remains virtually the same upon the addition of sodium, magnesium, potassium or calcium ions. This indicates that these metal ions do not significantly influence the secondary structure of Slt35. The intensity of the CD signal at 222 nm was used to follow the unfolding of Slt35, because α-helices have a maximal signal at this wavelength. In the absence of cations, Slt35 shows a sharp thermal transition stage from 46 to 50°C with the melting temperature T_m, the temperature at the midpoint of the transition curve, at 48°C (Fig. 3B). Addition of 10 mM sodium, magnesium, or potas-

Table 2
Comparison of native Slt35, Slt35-Na and Slt35-Ca

A. RMS differences (Å) for Cα atoms after superposition of indicated residues			
Structure 1	Structure 2	Residues 40–98, 109–361 (312 Cα atoms)	Residues 237–251 (15 Cα atoms)
native Slt35	Slt35-Na	0.13	0.09
native Slt35	Slt35-Ca	0.16	0.16
Slt35-Na	Slt35-Ca	0.14	0.19
B. Metal ion-metal ion distance after superposition of indicated residues (Å)			
Structure 1	Structure 2	Residues 40–98, 109–361 (312 Cα atoms)	Residue 237–251 (15 Cα atoms)
native Slt35	Slt35-Na	0.13	0.09
native Slt35	Slt35-Ca	0.75	0.69
Slt35-Na	Slt35-Ca	0.82	0.69

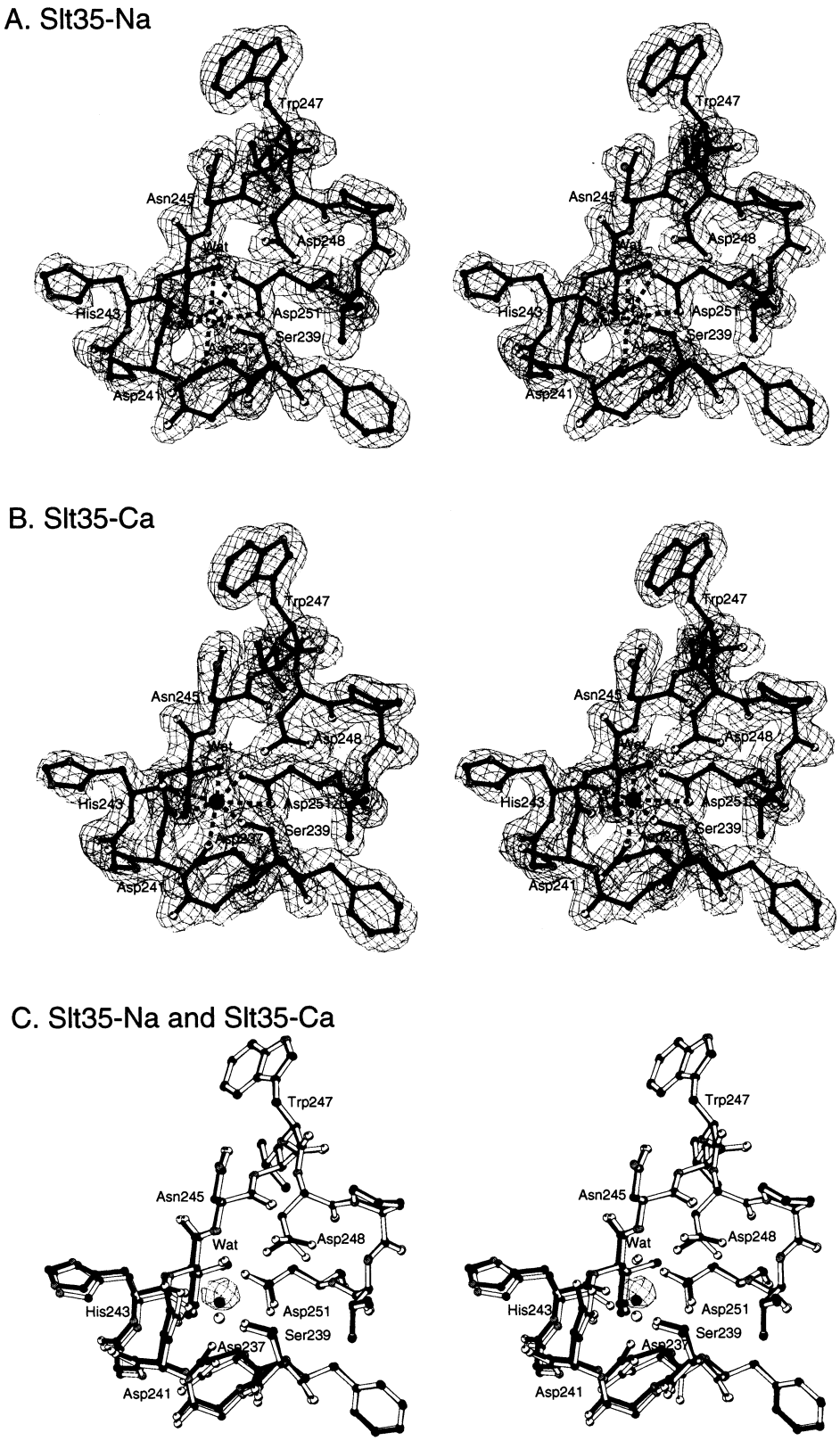

Fig. 2. Stereo views of the metal ion-binding site in Slt35. A: σ_A-weighted $2F_o-F_c$ electron density contoured at 1σ calculated from the final Slt35-Na model. B: σ_A-weighted $2F_o-F_c$ electron density contoured at 1σ calculated from the final Slt35-Ca model. C: Superposition of the metal ion-binding sites (residues 237–251) of Slt35-Na (white) and Slt35-Ca (black) using the Cα atoms. A σ_A-weighted $(|F_{obs}(Ca^{2+})|-|F_{obs}(Na^{+})|)$ electron density map contoured at 10σ (peak height is 22σ) is superimposed on the models. Phases derived from the final Slt35-Na model were used to calculate this electron density map. The nitrogen and oxygen atoms are respectively displayed in grey and white. The figure was prepared with BOBSCRIPT [24].

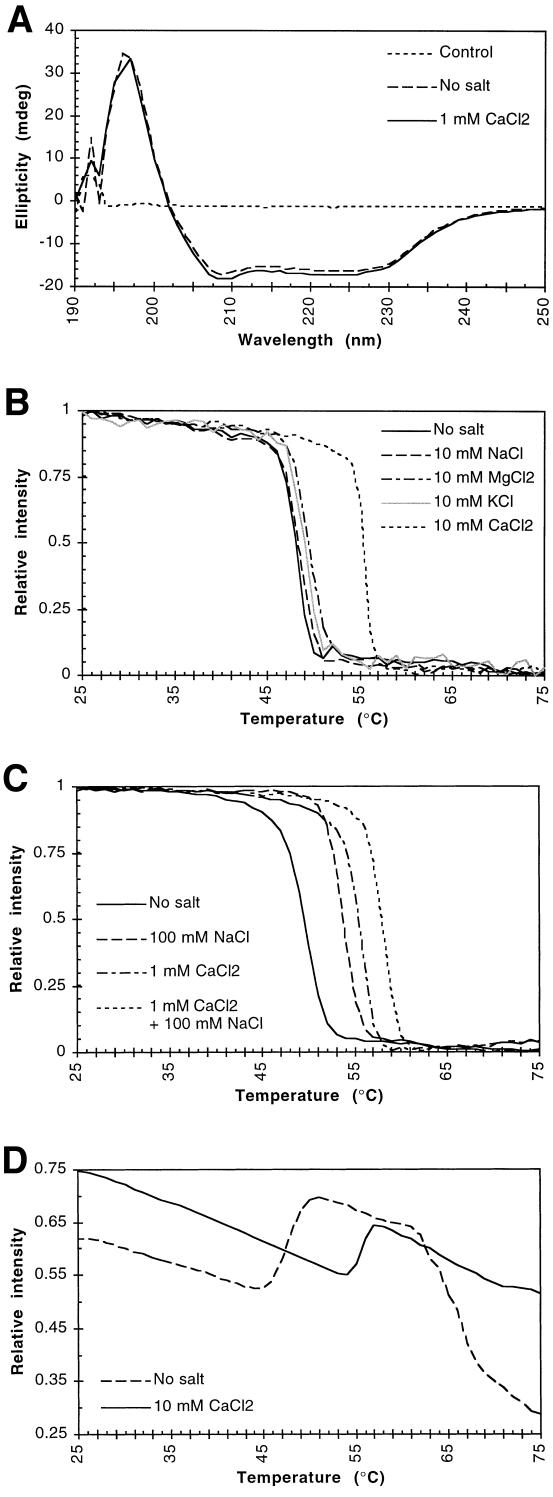

Fig. 3. CD and fluorescence spectroscopy studies on Slt35. A: CD spectra of Slt35 (70 μg/ml) in the absence or presence of 1 mM $CaCl_2$. The control sample consisted of 50 mM Tris-HCl, pH 7.4, and 2% isopropanol. B: Heat-induced unfolding of Slt35 in the absence or presence of 10 mM mono- and divalent ions as monitored by CD at 222 nm. C: Heat-induced unfolding of Slt35 in the absence or presence of 1 mM $CaCl_2$ with or without 100 mM NaCl as monitored by CD at 222 nm. D: Heat-induced unfolding of Slt35 monitored by fluorescence spectroscopy at 305–500 nm after excitation at 295 nm. In all experiments, the protein (70 μg/ml) was dissolved in 50 mM Tris-HCl, pH 7.4, and 2% isopropanol, in either the presence or absence of metal ions as indicated.

sium ions does not significantly affect the thermal transition stage. However, in the presence of 1 or 10 mM calcium, the melting temperature of Slt35 increases to about 55.5°C, indicating that calcium binds to Slt35 and improves its thermostability. Unfortunately, temperature backscans from 75 to 25°C showed that the heat-induced unfolding of Slt35 was irreversible. Even in the presence of 100 mM NaCl, 1 mM $CaCl_2$ still increases the enzyme's thermostability (T_m is 58°C compared to 53.5°C for 100 mM NaCl alone, see Fig. 3C). From this we conclude that the affinity of the enzyme for calcium ions is significantly higher than for sodium ions.

Heat-induced unfolding of Slt35 was also monitored by fluorescence spectroscopy. Fig. 3D shows that the thermal transition stages obtained by this method are in good agreement with the results from the CD experiments. Both techniques show that the thermostability of Slt35 is increased in the presence of calcium.

3.4. Function of the EF-hand in MltB transglycosylases

Amino acid sequence comparisons show that the EF-hand consensus sequence is conserved among the MltB transglycosylases (Fig. 4). This suggests that the EF-hand domain is of functional importance. Above we have shown that the EF-hand preferentially binds Ca^{2+} ions, and that Ca^{2+} ions increase the thermostability of the enzyme. Thus the EF-hand calcium-binding site of Slt35 is important for stability.

Nevertheless, other functions of the EF-hand domain may be possible. Eukaryotic proteins with multiple EF-hand calcium-binding domains often show conformational changes upon calcium binding, which is a crucial step in Ca^{2+}-dependent signal transduction [2]. Slt35 has only a single EF-hand domain, and the comparison of the Slt35-Na and Slt35-Ca structures did not reveal large structural differences, making a function in signal transduction unlikely. Furthermore, a direct role of the EF-hand domain in the reaction mechanism is also unlikely, since the calcium-binding site is ~20 Å from the active site and not close to any putative substrate-binding region.

In contrast, the exposed position of the EF-hand domain might allow it to interact with other proteins. It has been shown that Slt35 interacts with the penicillin-binding proteins 1B, 1C or 3 [20]. Unfortunately, it is not known which residues are involved in these interactions. Furthermore, the EF-hand domain could play a role in facilitating the folding of MltB after its translocation to the periplasm. A role in aiding folding has been proposed for the calcium-binding site in equine lysozyme [21], which has a fold resembling that of the core domain of Slt35, and which contains a calcium-binding site in a position similar to that of Slt35. As the calcium concentration in the periplasm is about 0.1–1 mM [22], this would be sufficient to stabilise the fold of Slt35. However, further research is required to unambiguously establish any other functional role for the EF-hand domain in the MltBs besides its importance for stability.

Acknowledgements: We thank Marcel de Vocht and Gea Schuurman-Wolters for their help with the circular dichroism and fluorescence measurements. We also thank Arnoud Dijkstra and Wolfgang Keck for stimulating discussions and ample supply of protein. The investigations were supported by the Netherlands Foundation for Chemical Research (SON) with financial aid from the Netherlands Organisation for Scientific Research (NWO).

EF-hand calcium-binding motif in MltB transglycosylases

```
                                        237            251
                                         | EF-hand motif |
Source                        225  <-H10->                <-----H11----->  265
Escherichia coli                QFMPSSYKQYAV DFSGDGHINLWD--PVD AIGSVANYFKAHGW
Yersinia pestis 1               QFMPSSFKRYAV DFDGNGHINLWD--PVD AIGSVANYFKSHGW
Yersinia pestis 2               QFMPSSFLTYGA DGDSDGKIDIWNN-IDD VFASTANYLSTQGW
Pseudomonas aeruginosa 1        QFMPSSFTKYAV DFDGDGHIDLWN--PRD AIGSVANYFKQHGW
Pseudomonas aeruginosa 2        QFMPSSFRAYAV DFDGDGHINIWSD-PTD AIGSVASYFKQHGW
Pseudomonas aeruginosa 3        QFIPTTHNQYAV DFDGDGKRDIWGS-PGD ALASTANYLKASGW
Pseudomonas aeruginosa 4        QFMPSTYARIAV DFDGDGRRDLVGS-VPD ALGSTANYLKKAGW
Neisseria gonorrhoeae (350)     QFMPSSYRKWAV DYDGDGHRDIWGN-VRD VAASVANYMKQHGW
Neisseria gonorrhoeae (248)     QFMPSSYRKWAV DYDGDGHRDIWGN-VGD VAASVANYMKQHGW
Neisseria meningitidis (sA)     QFMPSSYRKWAV DYDGDGHRDIWGN-VGD VAASIANYMKQHGW
Neisseria meningitidis MC58     QFMPSSYRKWAV DYDGDGHRDIWGN-VGD VAASVANYMKQHGW
H. actinomycetemcomitans        QFMPSSYLSYAA DGNNDGEKNIWTD-HYD VFASIANYLHTVGW
Rhodobacter sphaeroides         QFIPTSYLAYAV DFNGDGRRDIWSDDPTD ALASAAAYLSRSGW
                                **.*..       *    *   .      *    * * *    **
Coordination                                 X Y Z-Y-X      -Z
```

Fig. 4. Multiple sequence alignment of the EF-hand calcium-binding domains in MltB transglycosylases from various Gram-negative bacteria. Sequences were obtained via the BLAST server of the NCBI [25]. Residue labeling of the *E. coli* Slt35 and the α-helices H10 and H11 of Slt35 are indicated at the top of the figure. Residues at the X, Y, Z, −X, and −Z positions coordinate the metal ion with an oxygen atom of their side chain. The side chain of the −X residue is too short and the coordination occurs via a bridging water molecule. The −Y residue uses a main-chain carbonyl oxygen atom to coordinate the ion. The carboxylate at −Z coordinates the calcium ion with both oxygen atoms. X and −X define the unique axis of a pentagonal bipyramid [3]. Alignment of the sequences was done with the program CLUSTALW [26]. After the catalytic residues the EF-hand loop is the second most conserved region in the MltB transglycosylases.

Table 3
Geometry of the metal ion-binding sites in Slt35-Na and Slt35-Ca

A. Distances (Å) and *B*-factors (Å^2) of ligands to the metal ion

Data set			Slt35-Na		Slt35-Ca	
Coordination[b]	residue	atom	distance to ion (Å)	*B*-factor (Å^2)	distance to ion (Å)	*B*-factor (Å^2)
X	Asp-237	Oδ1	2.3	13	2.3	10
Y	Ser-239	Oγ	2.6	6	2.5	8
Z	Asp-241	Oδ1	2.4	7	2.4	8
−Y	His-243	O	2.3	9	2.4	11
−X	Water 574	OH2	(3.4)	(21)	2.4	9
$-Z_1$	Asp-251	Oδ1	2.6	11	2.7	11
$-Z_2$	Asp-251	Oδ2	2.6	12	2.5	11
	Averaged		2.45[a]	9.7[a]	2.46	9.7
	Metal ion		–	10	–	11

B. Significant differences in $\chi 1/\chi 2$ angles and ϕ/ψ angles in the EF-hand loop

Residue	$\chi 1/\chi 2$ angles in Slt35-Na	$\chi 1/\chi 2$ angles in Slt35-Ca
Asp-237	171/13	168/32
Asp-241	65/0	68/−22
Asp-248	176/−79	179/−29
Asp-251	−79/−14	−80/14
Residue	ϕ/ψ angles in Slt35-Na	ϕ/ψ angles in Slt35-Ca
Asp-237	−83/94	−86/74
His-243	−122/162	−123/139

[a]Water 574 is excluded from the averaging.
[b]See Fig. 4 for the definition of the coordination in the EF-hands.

References

[1] Kretsinger, R.H. and Nockolds, C.E. (1973) J. Biol. Chem. 248, 3313–3326.
[2] Ikura, M. (1996) Trends Biochem. Sci. 21, 14–17.
[3] Kretsinger, R. (1997) Nature Struct. Biol. 4, 514–516.
[4] Vyas, N.K., Vyas, M.N. and Quiocho, F.A. (1987) Nature 327, 635–638.
[5] Zou, J.Y., Flocco, M.M. and Mowbray, S.L. (1993) J. Mol. Biol. 233, 739–752.
[6] van Asselt, E.J., Perrakis, A., Kalk, K.H., Lamzin, V.S. and Dijkstra, B.W. (1998) Acta Crystallogr. D 54, 58–73.
[7] van Asselt, E.J., Dijkstra, A.J., Kalk, K.H., Takacs, B., Keck, W. and Dijkstra, B.W. (1999) Structure (in press).
[8] Dijkstra, A.J., Hermann, F. and Keck, W. (1995) FEBS Lett. 366, 115–118.
[9] Ehlert, K., Höltje, J.-V. and Templin, M.F. (1995) Mol. Microbiol. 16, 761–768.
[10] Höltje, J.-V. (1995) Arch. Microbiol. 164, 243–254.
[11] Dijkstra, A.J. and Keck, W. (1996) J. Bacteriol. 178, 5555–5562.
[12] Höltje, J.-V. and Tuomanen, E.I. (1991) J. Gen. Microbiol. 137, 441–454.
[13] Swain, A.L., Kretsinger, R.H. and Amma, E.L. (1989) J. Biol. Chem. 264, 16620–16628.
[14] Otwinowski, Z. and Minor, W. (1997) Methods Enzymol. 276, 307–326.
[15] Brünger, A.T. (1992) X-PLOR. A System for Crystallography and NMR, Yale University, New Haven, CT.
[16] Jones, T.A., Zou, J.-Y., Cowan, S.W. and Kjeldgaard, M. (1991) Acta Crystallogr. A 47, 110–119.
[17] Laskowski, R.A., MacArthur, M.W., Moss, D.S. and Thornton, J.M. (1993) J. Appl. Crystallogr. 26, 283–291.
[18] Vriend, G. and Sander, C. (1993) J. Appl. Crystallogr. 26, 47–60.
[19] Luck, L.A. and Falke, J.J. (1991) Biochemistry 30, 4257–4261.
[20] von Rechenberg, M., Ursinus, A. and Höltje, J.-V. (1996) Microb. Drug Resist. 2, 155–157.
[21] Morozova-Roche, L.A., Arico-Muendel, C.C., Haynie, D.T., Emelyanenko, V.I., Van Dael, H. and Dobson, C.M. (1997) J. Mol. Biol. 268, 903–921.
[22] Norris, V., Grant, S., Freestone, P., Canvin, J., Sheikh, F.N., Toth, I., Trinei, M., Modha, K. and Norman, R.I. (1996) J. Bacteriol. 178, 3677–3682.
[23] Kraulis, P.J. (1991) J. Appl. Crystallogr. 24, 946–950.
[24] Esnouf, R.M. (1997) J. Mol. Graph. 15, 133–138.
[25] Altschul, S.F., Madden, T.L., Schiffer, A.A., Zhang, J., Zhang, Z., Miller, W. and Lipman, D.J. (1997) Nucleic Acids Res. 25, 3389–3402.
[26] Thompson, J.D., Higgins, D.G. and Gibson, T.J. (1994) Nucleic Acids Res. 22, 4673–4680.
[27] Engh, R.A. and Huber, R. (1991) Acta Crystallogr. A 47, 392–400.